

Photoacoustic Vision for Surgical Guidance

(Invited Paper)

Muyinatu A. Lediju Bell*^{†‡},

*Department of Electrical and Computer Engineering, Johns Hopkins University, Baltimore, MD

[†]Department of Biomedical Engineering, Johns Hopkins University, Baltimore, MD

[‡]Department of Computer Science, Johns Hopkins University, Baltimore, MD

Abstract—Photoacoustic imaging offers “x-ray vision” to see beyond tool tips and underneath tissue during surgical procedures, without requiring ionizing x-rays. Instead, optical fibers and acoustic receivers enable photoacoustic sensing of major structures – like blood vessels and nerves – that are otherwise hidden from view. Laser pulses are transmitted through the optical fibers to illuminate regions of interest, causing an acoustic response that is detectable with ultrasound transducers. This invited contribution highlights a few applications of photoacoustic imaging for surgical guidance and connects novel light delivery systems introduced by the Photoacoustic & Ultrasonic Systems Engineering (PULSE) Lab to our newly developed coherence-based beamforming theory. The paper concludes with a vision statement describing possibilities for the usage of photoacoustic imaging in operating rooms and interventional suites.

I. INTRODUCTION

The fictitious concept of “x-ray vision” is widely understood to be the ability to see through structures that are not transparent to the human eye. This concept would be a useful feature for surgeons, particularly when navigating complex anatomy. The Photoacoustic & Ultrasonic Systems Engineering (PULSE) Lab is developing imaging systems to offer this capability [1], but not with ionizing x-rays. Instead, we are utilizing a different wavelength on the electromagnetic spectrum, specifically the nm wavelengths required to induce the photoacoustic effect and enable photoacoustic imaging [2]–[4] for surgical guidance to visualize metal tool tips and avoid accidental injury to major blood vessels or nerves.

The photoacoustic effect (i.e., the ability to convert optical energy to acoustic energy) was introduced by Alexander Graham Bell [5]–[7]. Many have since proposed and demonstrated the feasibility of using the photoacoustic effect to guide surgical and interventional procedures [1], [8]–[10]. Feasibility was initially demonstrated with minimally invasive procedures requiring tasks such as needle detection [11]–[13], biopsy guidance [11], [14], [15], and brachytherapy seed localization [16]–[18]. This concept was later expanded beyond these few initial cases to include more complex surgical and interventional examples, such as endonasal transsphenoidal surgeries of the skull base to remove pituitary tumors [19], [20], teleoperative surgeries performed with the da Vinci robot [21]–[23], cardiac catheterization and ablation procedures [24]–[27], and abdominal or pelvic surgeries [28]–[30].

The first practical step to leveraging the photoacoustic effect for surgical guidance is light transmission to a region interest. There are several possibilities for this light delivery, including

attachment of one or more optical fibers to catheter ultrasound transducers for endoscopy [31]–[33] or intravascular applications [34]–[36], insertion of optical fibers in needle or catheter tips [12], [13], [16], and external coupling to the tips of surgical tools [22], [37], [38]. Three possible attachment designs are featured in Fig. 1 for a scissor tool component of the da Vinci surgical system [22], a neurosurgical drill tip [37], and a mock spinal fusion surgery drill tip [38]. These three examples also show the unique light profiles produced by each design. In addition to being attached to surgical tools, light sources may also be operated independently of surgical tools.

After optical energy is transmitted to the photoacoustic target, the target absorbs the light, undergoes thermal expansion, and the photoacoustic signal is generated. The resulting acoustic energy, which can be sensed by an external ultrasound transducer external to the surgical site, must be converted into an image. Beamforming is one option for this conversion when the ultrasound transducer is comprised of an array of receive elements. The process from light delivery design to photoacoustic image formation is summarized in the top of Fig. 2.

Historically, amplitude-based beamforming and backprojection reconstructions methods have been applied to create photoacoustic images, which is advantageous when interested in quantitative details [39]. Beamforming is generally preferred over backprojection for surgical applications when ultrasound

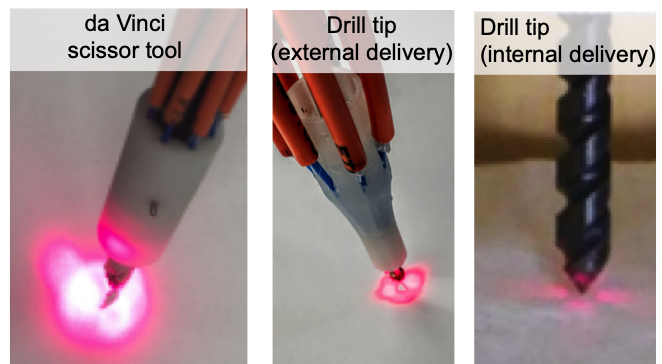


Fig. 1. Light profiles created from attachment of optical fiber(s) to surgical tools, demonstrating cases of external light delivery for a da Vinci scissor tool [22], external light delivery for a neurosurgical drill tip [37], and internal light delivery for a mock spinal fusion surgery drill tip [38].

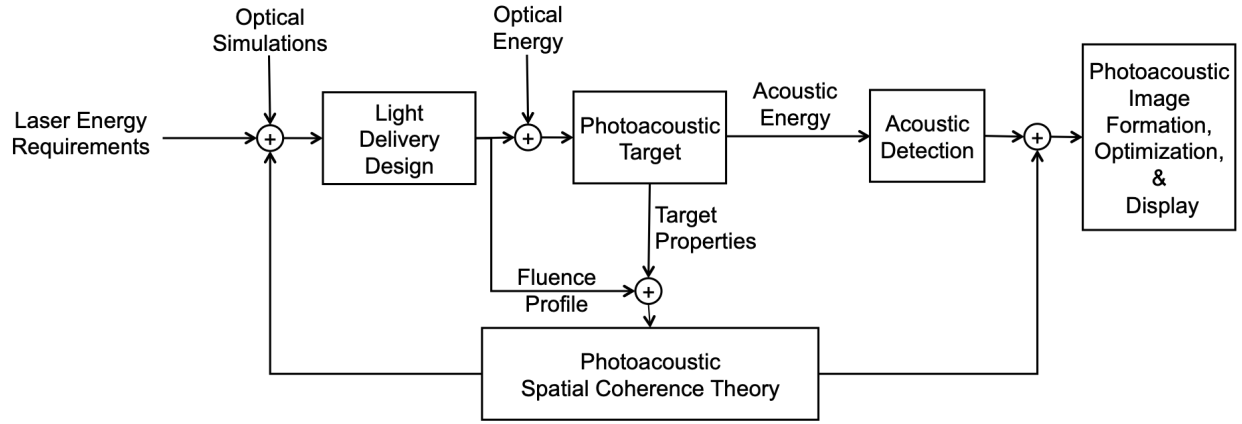


Fig. 2. Block diagram summarizing coherence-based photoacoustic system design elements and the associated imaging process. This diagram demonstrates that spatial coherence theory: (1) depends on fluence profiles and target properties and (2) impacts both light delivery and image formation.

probes are placed externally, which precludes effective use of ring arrays (i.e., spherical or cylindrical detection surfaces), which are more favorable for backprojection algorithms and quantitative photoacoustic applications. Amplitude-based beamforming is also useful when detecting major blood vessels in the *in vivo* liver, as more focused signals were previously observed when the transmitted light was in the direct line of sight of a major vessel and diffuse signals were observed otherwise [28]. This difference is a direct result of the amplitude-based beamforming process, which focuses the received acoustic energy to a fixed point in space, and the amplitude of the focused energy is maximized with amplitude-based beamforming. Amplitude-based beamforming has also been useful to determine distance from major blood vessels that need to be avoided during surgery [20].

Despite the requirement for amplitude-based beamforming to achieve some surgical and interventional tasks, most applications of photoacoustic imaging for surgical guidance do not require amplitude information. Instead, the main goal is to provide surgeons with the best contrast to visualize targets of interest, particularly for low-energy laser systems (e.g., pulsed laser diodes), which are smaller and more portable than higher-energy systems. These low-energy light delivery systems are often more suitable for interventional or surgical use due to their smaller footprints, and their utility can be enhanced with a coherence-based photoacoustic beamforming approach [40].

This invited contribution is organized as follows. Section II connects novel light delivery systems developed by the PULSE Lab [22], [37], [38] to newly developed spatial coherence theory introduced by Graham and Bell [41], as summarized in Fig. 2. Section III describes possible applications of this theory for surgical guidance techniques. Section IV concludes the paper with a vision for photoacoustic-guided surgery in operating rooms and interventional suites.

II. PHOTOACOUSTIC SPATIAL COHERENCE THEORY

Spatial coherence theory was recently developed to describe the governing principles of coherence-based photoacoustic

beamforming and image optimization [41]–[43]. This theory can be thought of as the van Cittert Zernike theorem [44] (which predicts the spatial covariance of a wave field produced by an incoherent source) applied to photoacoustic data. The requirement for an incoherent source is satisfied by modeling a photoacoustic target (e.g., a blood vessel) as a random distribution of spatially incoherent absorbers, resulting in the expression:

$$\mathcal{C}(u, v) = \frac{1}{z^2} \int_{-\infty}^{\infty} \int_{-\infty}^{\infty} [\chi_o |\mu_a \Gamma F|^2 + 2\chi_o N_A \langle \Gamma \mu_a F \rangle + \chi_o N_o |\langle \Gamma \mu_a F \rangle|^2] e^{-j2\pi(ux+vy)} dx dy, \quad (1)$$

where \mathcal{C} represents the spatial covariance in the spatial frequency domain, u and v are spatial frequencies in the lateral and elevation ultrasound receiver dimensions, respectively, χ_o is the average power of the absorber distribution, μ_a and Γ are the photoacoustic target properties of optical absorption and Grüneisen parameter, respectively, and F is the laser fluence at a depth of interest, z . Although the spatial dependency on (x, y) coordinates is not shown in Eq. 1, the terms μ_a , Γ , and F can each vary in these spatial dimensions. The remaining terms in Eq. 1 are noise terms introduced by uncorrelated source-related noise originating from random fluctuations in the source distribution (e.g., variations in fluence at the absorber surface [45] and variations in the optical absorption within each absorber). This additive noise model was developed based on observations of experimental data [45]. Specifically, N_A is zero-mean, Gaussian distributed, additive noise, and N_o is the variance of this additive noise.

When noise is absent, Eq. 1 reduces to:

$$\mathcal{C}(u, v) = \frac{1}{z^2} \int_{-\infty}^{\infty} \int_{-\infty}^{\infty} \chi_o |\Gamma \mu_a F|^2 e^{-j2\pi(ux+vy)} dx dy. \quad (2)$$

Eq. 2 can be compared to the familiar van Cittert Zernike theorem applied to pulse-echo ultrasound measurements, rep-

resented as [46], [47]:

$$\mathcal{C}(u, v) = \frac{1}{z^2} \int_{-\infty}^{\infty} \int_{-\infty}^{\infty} |\chi(x, y) H(x, y)|^2 e^{-j2\pi(ux+vy)} dx dy, \quad (3)$$

where $\chi(x, y)$ is the source function, and $H(x, y)$ is the transmit beam amplitude. Although Eqs. 1-3 each contain a source term (i.e., $A(x, y) = \mu_a \Gamma F$ can be considered as the photoacoustic source term), note that the $H(x, y)$ term in the ultrasound expression of Eq. 3 does not exist in the photoacoustic expressions of Eqs. 1 and 2 because there are no transmit ultrasound beams in photoacoustic imaging. Instead, the receive beam steering required to make photoacoustic images is described by a multiplicative phase term to the Fourier transform expressions in Eqs. 1 and 2, which produces the following expression in the separable lateral ultrasound transducer dimension:

$$\mathcal{C}(u, x_k) = \frac{e^{-j2\pi x_k u}}{z^2} \int_{-\infty}^{\infty} [\chi_o |\Gamma \mu_a F|^2 + 2\chi_o N_A (\Gamma \mu_a F)^2 + \chi_o N_o |\langle \Gamma \mu_a F \rangle|^2] e^{-j2\pi x u} dx, \quad (4)$$

where x_k is a lateral focal point in the final image (i.e., after beam steering).

The spatial frequency, u , in Eqs. 1-4 is related to spatial lag, m , through the expression:

$$u = \frac{m}{\lambda z} \quad (5)$$

where m is the spatial distance between two gridpoints on an aperture receiving an acoustic response, and λ represents an acoustic frequency associated with the ultrasound transducer. Based on this relationship, Eq. 3 or 4 is then integrated up to the first M spatial lags to achieve one ultrasound short-lag spatial coherence (SLSC) image pixel [47] or one photoacoustic SLSC image pixel (after accounting for spectral bandwidth) [41], respectively. This process is repeated to build theoretical ultrasound and photoacoustic SLSC images.

Common adjustments and optimizations to SLSC images created from experimental data include altering the M value for the integration step [47]–[52] or the kernel length of correlated data [53]–[56] in efforts to achieve the best contrast, resolution, and real-time implementations in both ultrasound and photoacoustic SLSC images. However, considering the additional number of terms in Eq. 4 compared to Eq. 3, there are additional variables that can be exploited to optimize coherence-based photoacoustic image contrast and resolution.

III. APPLICATIONS OF PHOTOACOUSTIC SPATIAL COHERENCE THEORY TO SURGICAL GUIDANCE

Fig. 2 shows the impact of photoacoustic spatial coherence theory on both image formation and light delivery designs. In most applications of surgical guidance, the endogenous photoacoustic targets within a patient (e.g., blood vessels) will not be modified, leaving light delivery as one of the major design elements. Light delivery designs are generally dictated by laser safety standards [57], which report fluence limits based on laser wavelengths and pulse energies. As fluence is often defined as the ratio of energy to incident surface area, one option to maximize the input optical energy within laser safety limits is to increase the available surface area (while maintaining the small form factor of minimally invasive surgical devices), as previously demonstrated using a series of optical simulation software [37].

In addition to the optical design component described above, five applications of the newly developed photoacoustic spatial coherence theory that affect both light delivery designs and image formation are described in [41], illustrated in Fig. 3, and summarized below. First, the photoacoustic target may be incorporated as an additional design element if we consider that there are multiple options to attach specialized light delivery systems to the tips of various surgical tools, with each option generating a unique light profile (as shown in Fig. 1) and a unique photoacoustic response from the tool tip. From this perspective, the first possible application is that spatial coherence theory can be used to optimize light delivery designs [20], [22], [37]. More specifically, Fig. 2 and Eqs. 1, 2, and 4 indicate that this theory can be used to determine how

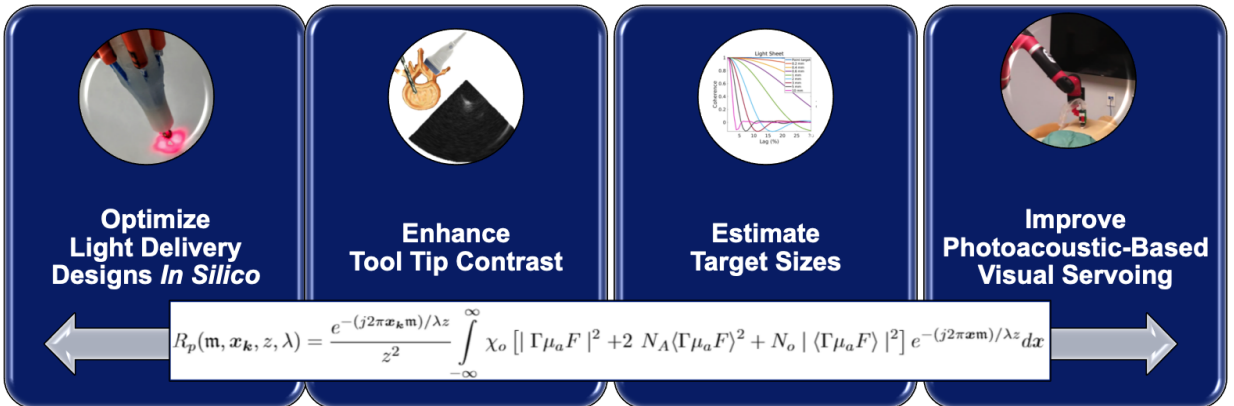


Fig. 3. Summary of potential applications for photoacoustic spatial coherence theory to guide surgical and interventional procedures.

the fluence associated with various light profile designs at a particular axial depth of interest (i.e., z) affects SLSC image contrast and resolution *in silico*, as demonstrated in [41].

The second application is that spatial coherence theory can be used to enhance tool tip contrast in photoacoustic images for surgical guidance (e.g., drill tips during spinal fusion surgery [38], fiber tips during real-time visual servoing [56], catheter or needle tips during interventional procedures [24], [58]). This optimization can be achieved by choosing which M value will be used to display images based on *a priori* information about expected target sizes (e.g., tool tips, metal implants such as brachytherapy seeds, average sizes of major arteries to be avoided within a specific anatomical location). This image display choice can also be achieved by incorporating knowledge of expected light profiles at the depth of the photoacoustic target of interest.

Third, the newly developed photoacoustic spatial coherence theory can be used to estimate target sizes based on spatial coherence functions. Generally, coherence length is correlated with the size of a target when a light profile illuminates the entirety of a target to generate the photoacoustic effect. Otherwise, if the size of the target is larger than the size of the light profile, the size of the light profile dictates the coherence length (see Fig. 6 in [41]). This information can potentially be used to estimate target sizes (or light profile sizes in the latter case) by measuring coherence length from delayed photoacoustic channel data, without requiring any image formation.

Fourth, spatial coherence theory can be used to improve real-time photoacoustic-based robotic visual servoing of surgical tool tips, as demonstrated by Gonzalez and Bell [56]. Visual servoing is a robot control strategy that uses computer vision to find and stay centered on targets of interest. In photoacoustic-based visual servoing, the computer vision is provided by photoacoustic images. This approach is useful to relieve interventionalists from finding and remaining centered on photoacoustic signals associated with the tips of needles, catheters, or optical fibers attached to other surgical tools [24], [58], [59]. Instead, a robot arm holding an ultrasound probe would be tasked with this important responsibility. The robot, ultrasound, and laser systems utilized to achieve photoacoustic-based visual servoing would ideally be as small as possible to avoid being obtrusive in the operating room or interventional suite [1]. Smaller laser systems typically provide lower laser energies, which reduces the overall signal-to-noise ratio of the imaging system. The contrast of photoacoustic images can be boosted in these cases with the application of coherence-based beamforming rather than more traditional amplitude-based beamforming approaches [40], [56].

Finally, although much of the presented theory was developed and demonstrated in the context of SLSC imaging, this theory can be applied and extended to any photoacoustic method that utilizes spatial coherence. Other possibilities include applications in coherence-based cell tracking, blood flow measurements, and other coherence-based beamforming methods.

IV. CONCLUSION

While x-ray vision is a fictitious idea, photoacoustic imaging for surgical guidance is not such a far-fetched concept. The overall vision for this concept requires light transmission to a surgical site of interest. This transmission can be accomplished with optical fibers attached to surgical tools or operated independently of surgical tools. The resulting photoacoustic effect produced within structures of interest, such as major blood vessels or nerves to be avoided during surgery, can be detected with conventional ultrasound transducers that are placed externally to avoid interference with the surgical site. Depending on the surgery, this concept can also be achieved with the more traditional approach of attaching light sources to ultrasound transducers, which is particularly true of endoscopic or catheter-based ultrasound devices. Beamforming plays a critical role in the quality of provided images, with both amplitude-based and coherence-based offering independent, yet equally important benefits.

Once developed and optimized for a specific surgical task, the entire photoacoustic imaging system may additionally be integrated with surgical robots to enhance computer vision capabilities during robotic surgeries. Similarly, these photoacoustic imaging assistants can be coupled with medical robots to improve maneuverability, autonomy, and operability of imaging system components or to improve image interpretation during surgeries and other interventional procedures. For specific surgical and interventional cases, the photoacoustic imaging systems would ideally be miniaturized versions of the current systems available today, which would require additional innovations in sensing technology, image quality improvements, and modifications to current laser safety definitions, as discussed in more detail in [1].

ACKNOWLEDGMENTS

This work is supported by NSF CAREER Award ECCS-1751522, NSF SCH Award IIS-2014088, and NIH R00-EB018994.

REFERENCES

- [1] M. A. Lediju Bell, "Photoacoustic imaging for surgical guidance: Principles, applications, and outlook," *Journal of Applied Physics*, vol. 128, no. 6, p. 060904, 2020.
- [2] P. Beard, "Biomedical photoacoustic imaging," *Interface Focus*, vol. 1, no. 4, pp. 602–631, 2011.
- [3] R. Bouchard, O. Sahin, and S. Emelianov, "Ultrasound-guided photoacoustic imaging: current state and future development," *IEEE Transactions on Ultrasonics, Ferroelectrics, and Frequency Control*, vol. 61, no. 3, pp. 450–466, 2014.
- [4] M. Xu and L. V. Wang, "Photoacoustic imaging in biomedicine," *Review of Scientific Instruments*, vol. 77, no. 4, p. 041101, 2006.
- [5] A. G. Bell, "Upon the production and reproduction of sound by light," *Journal of the Society of Telegraph Engineers*, vol. 9, no. 34, pp. 404–426, 1880.
- [6] —, "On the production and reproduction of sound by light," in *Proc. Am. Assoc. Adv. Sci.*, vol. 29, 1881, pp. 115–136.
- [7] —, *Upon the production of sound by radiant energy*. Gibson Brothers, printers, 1881.
- [8] M. S. Karthikesh and X. Yang, "Photoacoustic image-guided interventions," *Experimental Biology and Medicine*, vol. 245, no. 4, pp. 330–341, 2020.

- [9] T. Zhao, A. E. Desjardins, S. Ourselin, T. Vercauteren, and W. Xia, "Minimally invasive photoacoustic imaging: Current status and future perspectives," *Photoacoustics*, vol. 16, p. 100146, 2019.
- [10] I. Steinberg, D. M. Huland, O. Vermesh, H. E. Frostig, W. S. Tummers, and S. S. Gambhir, "Photoacoustic clinical imaging," *Photoacoustics*, vol. 14, pp. 77–98, 2019.
- [11] K. H. Song, E. W. Stein, J. A. Margenthaler, and L. V. Wang, "Noninvasive photoacoustic identification of sentinel lymph nodes containing methylene blue in vivo in a rat model," *Journal of Biomedical Optics*, vol. 13, no. 5, p. 054033, 2008.
- [12] D. Piras, C. Grijsen, P. Schutte, W. Steenbergen, and S. Manohar, "Photoacoustic needle: minimally invasive guidance to biopsy," *Journal of Biomedical Optics*, vol. 18, no. 7, p. 070502, 2013.
- [13] W. Xia, D. I. Nikitichev, J. M. Mari, S. J. West, R. Pratt, A. L. David, S. Ourselin, P. C. Beard, and A. E. Desjardins, "Performance characteristics of an interventional multispectral photoacoustic imaging system for guiding minimally invasive procedures," *Journal of Biomedical Optics*, vol. 20, no. 8, p. 086005, 2015.
- [14] C. Kim, T. N. Erpelding, K. I. Maslov, L. Jankovic, W. J. Akers, L. Song, S. Achilefu, J. A. Margenthaler, M. D. Pashley, and L. V. Wang, "Handheld array-based photoacoustic probe for guiding needle biopsy of sentinel lymph nodes," *Journal of Biomedical Optics*, vol. 15, no. 4, p. 046010, 2010.
- [15] K. Sivasubramanian, V. Periyasamy, and M. Pramanik, "Non-invasive sentinel lymph node mapping and needle guidance using clinical handheld photoacoustic imaging system in small animal," *Journal of Biophotonics*, vol. 11, no. 1, p. e201700061, 2018.
- [16] M. A. L. Bell, N. P. Kuo, D. Y. Song, J. U. Kang, and E. M. Boctor, "In vivo visualization of prostate brachytherapy seeds with photoacoustic imaging," *Journal of Biomedical Optics*, vol. 19, no. 12, pp. 126011–126011, 2014.
- [17] M. A. L. Bell, X. Guo, D. Y. Song, and E. M. Boctor, "Transurethral light delivery for prostate photoacoustic imaging," *Journal of Biomedical Optics*, vol. 20, no. 3, p. 036002, 2015.
- [18] J. L. Su, R. R. Bouchard, A. B. Karpiouk, J. D. Hazle, and S. Y. Emelianov, "Photoacoustic imaging of prostate brachytherapy seeds," *Biomedical Optics Express*, vol. 2, no. 8, pp. 2243–2254, 2011.
- [19] M. A. L. Bell, A. K. Ostrowski, K. Li, P. Kazanzides, and E. M. Boctor, "Localization of transcranial targets for photoacoustic-guided endonasal surgeries," *Photoacoustics*, vol. 3, no. 2, pp. 78–87, 2015.
- [20] M. Graham, J. Huang, F. Creighton, and M. A. L. Bell, "Simulations and human cadaver head studies to identify optimal acoustic receiver locations for minimally invasive photoacoustic-guided neurosurgery," *Photoacoustics*, vol. 19, p. 100183, 2020. [Online]. Available: <https://doi.org/10.1016/j.pacs.2020.100183>
- [21] N. Gandhi, M. Allard, S. Kim, P. Kazanzides, and M. A. L. Bell, "Photoacoustic-based approach to surgical guidance performed with and without a da vinci robot," *Journal of Biomedical Optics*, vol. 22, no. 12, p. 121606, 2017.
- [22] M. Allard, J. Shubert, and M. A. L. Bell, "Feasibility of photoacoustic-guided teleoperated hysterectomies," *Journal of Medical Imaging*, vol. 5, no. 2, p. 021213, 2018. [Online]. Available: <https://doi.org/10.1117/1.JMI.5.2.021213>
- [23] H. Moradi, S. Tang, and S. E. Salcudean, "Toward Robot-Assisted Photoacoustic Imaging: Implementation Using the da Vinci Research Kit and Virtual Fixtures," *IEEE Robotics and Automation Letters*, vol. 4, no. 2, pp. 1807–1814, 2019.
- [24] M. Graham, F. Assis, D. Allman, A. Wiacek, E. Gonzalez, M. Gubbi, J. Dong, H. Hou, S. Beck, J. Chrispin, and M. A. L. Bell, "In vivo demonstration of photoacoustic image guidance and robotic visual servoing for cardiac catheter-based interventions," *IEEE Transactions on Medical Imaging*, vol. 39, no. 4, pp. 1015–1029, 2020. [Online]. Available: <https://doi.org/10.1109/TMI.2019.2939568>
- [25] M. T. Graham, F. Assis, D. Allman, A. Wiacek, E. Gonzalez, M. R. Gubbi, J. Dong, H. Hou, S. Beck, J. Chrispin, and M. A. L. Bell, "Photoacoustic image guidance and robotic visual servoing to mitigate fluoroscopy during cardiac catheter interventions," in *Advanced Biomedical and Clinical Diagnostic and Surgical Guidance Systems XVIII*, vol. 11229. International Society for Optics and Photonics, 2020, p. 112291E.
- [26] S. Iskander-Rizk, A. F. van der Steen, and G. Van Soest, "Photoacoustic imaging for guidance of interventions in cardiovascular medicine," *Physics in Medicine & Biology*, vol. 64, no. 16, p. 16TR01, 2019.
- [27] A. F. Samdani, A. Ranade, D. M. Sciubba, P. J. Cahill, M. D. Antonacci, D. H. Clements, and R. R. Betz, "Accuracy of free-hand placement of thoracic pedicle screws in adolescent idiopathic scoliosis: how much of a difference does surgeon experience make?" *European Spine Journal*, vol. 19, no. 1, pp. 91–95, 2010.
- [28] K. M. Kempfski, A. Wiacek, M. Graham, E. González, B. Goodson, D. Allman, J. Palmer, H. Hou, S. Beck, J. He, and M. A. L. Bell, "In vivo photoacoustic imaging of major blood vessels in the pancreas and liver during surgery," *Journal of Biomedical Optics*, vol. 24, no. 12, p. 121905, 2019.
- [29] A. Wiacek, K. C. Wang, H. Wu, and M. A. L. Bell, "Dual-wavelength photoacoustic imaging for guidance of hysterectomy procedures," in *Advanced Biomedical and Clinical Diagnostic and Surgical Guidance Systems XVIII*, vol. 11229. International Society for Optics and Photonics, 2020, p. 112291D.
- [30] W. Xia, E. Maneas, D. I. Nikitichev, C. A. Mosse, G. S. Dos Santos, T. Vercauteren, A. L. David, J. Deprest, S. Ourselin, P. C. Beard, and A. Desjardins, "Interventional photoacoustic imaging of the human placenta with ultrasonic tracking for minimally invasive fetal surgeries," in *International Conference on Medical Image Computing and Computer-Assisted Intervention*. Springer, 2015, pp. 371–378.
- [31] J.-M. Yang, K. Maslov, H.-C. Yang, Q. Zhou, K. K. Shung, and L. V. Wang, "Photoacoustic endoscopy," *Optics Letters*, vol. 34, no. 10, pp. 1591–1593, 2009.
- [32] Y. Li, Z. Zhu, J. C. Jing, J. J. Chen, A. E. Heidari, Y. He, J. Zhu, T. Ma, M. Yu, Q. Zhou *et al.*, "High-speed integrated endoscopic photoacoustic and ultrasound imaging system," *IEEE Journal of Selected Topics in Quantum Electronics*, vol. 25, no. 1, pp. 1–5, 2018.
- [33] H. Lei, L. A. Johnson, K. A. Eaton, S. Liu, J. Ni, X. Wang, P. D. Higgins, and G. Xu, "Characterizing intestinal strictures of Crohn's disease in vivo by endoscopic photoacoustic imaging," *Biomedical Optics Express*, vol. 10, no. 5, pp. 2542–2555, 2019.
- [34] K. Jansen, A. F. Van Der Steen, H. M. van Beusekom, J. W. Oosterhuis, and G. van Soest, "Intravascular photoacoustic imaging of human coronary atherosclerosis," *Optics Letters*, vol. 36, no. 5, pp. 597–599, 2011.
- [35] B. Wang, J. L. Su, A. B. Karpiouk, K. V. Sokolov, R. W. Smalling, and S. Y. Emelianov, "Intravascular photoacoustic imaging," *IEEE Journal of Selected Topics in Quantum Electronics*, vol. 16, no. 3, pp. 588–599, 2010.
- [36] A. B. Karpiouk, B. Wang, and S. Y. Emelianov, "Development of a catheter for combined intravascular ultrasound and photoacoustic imaging," *Review of Scientific Instruments*, vol. 81, no. 1, p. 014901, 2010.
- [37] B. Eddins and M. A. L. Bell, "Design of a multifiber light delivery system for photoacoustic-guided surgery," *Journal of Biomedical Optics*, vol. 22, no. 4, p. 041011, 2017.
- [38] J. Shubert and M. A. L. Bell, "A novel drill design for photoacoustic guided surgeries," in *Photons Plus Ultrasound: Imaging and Sensing 2018*, vol. 10494. International Society for Optics and Photonics, 2018, p. 104940J.
- [39] A. Rosenthal, V. Ntziachristos, and D. Razansky, "Acoustic inversion in optoacoustic tomography: A review," *Current Medical Imaging*, vol. 9, no. 4, pp. 318–336, 2013.
- [40] M. A. L. Bell, X. Guo, H. J. Kang, and E. Boctor, "Improved contrast in laser-diode-based photoacoustic images with short-lag spatial coherence beamforming," in *2014 IEEE International Ultrasonics Symposium*. IEEE, 2014, pp. 37–40.
- [41] M. Graham and M. A. L. Bell, "Photoacoustic spatial coherence theory and applications to coherence-based image contrast and resolution," *IEEE Transactions on Ultrasonics, Ferroelectrics, and Frequency Control (accepted)*, 2020.
- [42] M. T. Graham and M. A. L. Bell, "Theoretical application of short-lag spatial coherence to photoacoustic imaging," in *IEEE International Ultrasonics Symposium*, 2017.
- [43] —, "Development and validation of a short-lag spatial coherence theory for photoacoustic imaging," in *Photons Plus Ultrasound: Imaging and Sensing 2018*, vol. 10494. International Society for Optics and Photonics, 2018, p. 104945K.
- [44] J. W. Goodman, *Statistical Optics*. John Wiley & Sons, 2015.
- [45] B. Stephanian, M. T. Graham, H. Hou, and M. A. L. Bell, "Additive noise models for photoacoustic spatial coherence theory," *Biomedical Optics Express*, vol. 9, no. 11, pp. 5566–5582, 2018.

- [46] R. Mallart and M. Fink, "The van Cittert-Zernike theorem in pulse echo measurements," *The Journal of the Acoustical Society of America*, vol. 90, no. 5, pp. 2718–2727, 1991.
- [47] M. A. Lediju Bell, G. E. Trahey, B. C. Byram, and J. J. Dahl, "Short-lag spatial coherence of backscattered echoes: Imaging characteristics," *IEEE Transactions on Ultrasonics, Ferroelectrics, and Frequency Control*, vol. 58, no. 7, pp. 1377–1388, 2011.
- [48] M. A. L. Bell, N. Kuo, D. Y. Song, and E. M. Boctor, "Short-lag spatial coherence beamforming of photoacoustic images for enhanced visualization of prostate brachytherapy seeds," *Biomedical Optics Express*, vol. 4, no. 10, pp. 1964–1977, 2013.
- [49] B. Pourebrahimi, S. Yoon, D. Dopsa, and M. C. Kolios, "Improving the quality of photoacoustic images using the short-lag spatial coherence imaging technique," in *Photons Plus Ultrasound: Imaging and Sensing 2013*, vol. 8581. International Society for Optics and Photonics, 2013, p. 85813Y.
- [50] J. J. Dahl, D. Hyun, M. A. Lediju, and G. E. Trahey, "Lesion detectability in diagnostic ultrasound with short-lag spatial coherence imaging," *Ultrasonic Imaging*, vol. 33, no. 2, pp. 119–133, 2011.
- [51] J. Dahl, D. Hyun, Y. Li, M. Jakovljevic, M. A. L. Bell, W. Long, N. Bottenus, V. Kakkad, and G. Trahey, "Coherence beamforming and its applications to the difficult-to-image patient," in *Proceedings of the 2017 IEEE International Ultrasonics Symposium, Washington, DC*, 2017.
- [52] A. A. Nair, T. D. Tran, and M. A. L. Bell, "Robust short-lag spatial coherence imaging," *IEEE transactions on Ultrasonics, Ferroelectrics, and Frequency Control*, vol. 65, no. 3, pp. 366–377, 2018.
- [53] M. A. Lediju Bell, J. J. Dahl, and G. E. Trahey, "Resolution and Brightness Characteristics of Short-Lag Spatial Coherence (SLSC) Images," *IEEE Transactions on Ultrasonics, Ferroelectrics, and Frequency Control*, vol. 62, no. 7, pp. 1265–1276, 2015.
- [54] D. Hyun, A. L. C. Crowley, and J. J. Dahl, "Efficient strategies for estimating the spatial coherence of backscatter," *IEEE Transactions on Ultrasonics, Ferroelectrics, and Frequency Control*, vol. 64, no. 3, pp. 500–513, 2016.
- [55] K. Kempinski, M. Graham, M. Gubbi, T. Palmer, and M. A. L. Bell, "Application of the generalized contrast-to-noise ratio to assess photoacoustic image quality," *Biomedical Optics Express*, vol. 11, no. 7, pp. 3684–3698, 2020.
- [56] E. Gonzalez and M. A. L. Bell, "GPU implementation of photoacoustic short-lag spatial coherence imaging for improved image-guided interventions," *Journal of Biomedical Optics*, 2020.
- [57] Laser Institute of America, "American national standards for safe use of lasers," *ANSI Z136.1-2014*, 2014.
- [58] M. A. L. Bell and J. Shubert, "Photoacoustic-based visual servoing of a needle tip," *Scientific Reports*, vol. 8, no. 1, p. 15519, 2018.
- [59] J. Shubert and M. A. L. Bell, "Photoacoustic based visual servoing of needle tips to improve biopsy on obese patients," in *IEEE International Ultrasonics Symposium*, 2017.